

RESEARCH ARTICLE

Study on the impact of different friction coefficient combinations of disc spring assemblies on load

Y. Ma^{1*}, S. Li¹, T. Su¹, Q. Yuan², Z. Song², X. Li³

¹ School of Mechanical Engineering and Automation, Liaoning University of Technology, Jinzhou 121001, China

² Zhongliao Testing (Liaoning) Co., Ltd, Shenyang, 110000, China

³ Liaoning Petrochemical Vocational and Technical College, Jinzhou, Liaoning, 121001, China

ABSTRACT - This paper focuses on the disc spring assembly in a certain type of disc spring bellows as the research object. According to the technical requirements of the bellows, disc spring assemblies with different combinations (face-to-face, stacked, and composite) are designed. The influence of the number of discs and different combinations on the load of disc spring assemblies with different friction coefficients is analyzed using numerical simulation methods and verified by experiments. The simulation results show that the number of discs in the face-to-face combination has no effect on the load, the number of discs in the stacked combination has a linearly increasing effect on the load, and the number of discs in the composite combination has a non-linear effect on the load. Furthermore, the numerical calculation results of the load with friction coefficients of 0, 0.1, and 0.16 are compared with the experimental results. The relative errors between the two results are 3.3%, 1.5%, and 1.4%, respectively, and the error values are within the allowable range, which verifies the accuracy of the load calculation model. After discussing the combination methods, finally, through comparative analysis, the load model of the composite disc spring structure is used to fit a prediction model of the number of discs and the load considering the influence of friction, which provides a theoretical reference for the engineering application of disc spring assemblies in disc spring bellows.

ARTICLE HISTORY

Received : 22nd Nov. 2024

Revised : 19th Jan. 2025

Accepted : 19th Feb. 2025

Published : 30th Mar. 2025

KEYWORDS

Disc spring

Belleville spring

Combination method

Configuration

Friction coefficient

Load

1. INTRODUCTION

A disc spring is a type of spring with a conical cross-section and washer form, as shown in Figure 1 with different numbers of stacked disc springs. Disc springs are notable for their strong load-bearing capacity, short stroke, small installation space requirements, and suitability for high-temperature working environments [1]. They are widely used in mechanical engineering and have largely replaced traditional coil springs, leading to extensive research on their various properties in both theoretical and engineering fields [2]. Due to the deformation or load-bearing capacity of single disc springs usually not meeting practical requirements, they are generally used in stacked, juxtaposed, or composite forms. Stacking increases load-bearing capacity, juxtaposition enhances deformation, and composite usage improves both load-bearing and deformation capacities. Currently, research on single disc springs is relatively sufficient, but the use of composite disc springs is more common in engineering, yet existing studies are scarce. Based on this, this paper intends to study the composite disc springs in disc spring bellows.

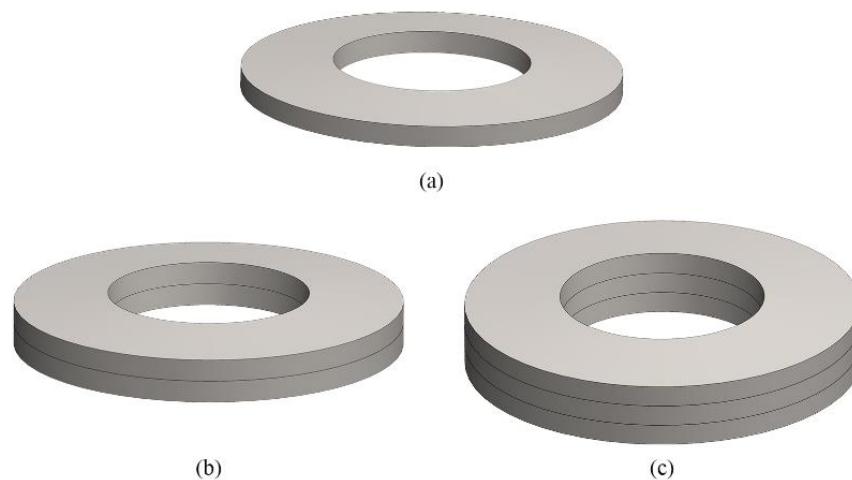


Figure 1. Different numbers of stacked disc springs in various combinations: (a) Single disc springs, (b) Double disc spring and (c) Triple disc spring

Almen and Laszlo [3] were the first to propose a solution for the load-displacement analysis of disc springs. Their study was based on the assumption that the cross-section of the disc spring does not deform during compression and rotates around its neutral point. Curti and Montanini [4] determined the characteristics of steel disc springs through experiments and finite element analysis using the Almen-Laszlo method and designed composite disc springs. Their comparison revealed that the properties of composite disc springs are comparable to or better than those of steel disc springs. Ozaki et al. [5] highlighted the importance of the friction effect between disc springs and support surfaces, leading them to derive a load-deflection formula for disc springs considering friction and noting that friction causes hysteresis during loading and unloading. Mastricola et al. [6] built a single disc spring model based on the torque balance method and extended Curti's equations to asymmetric friction conditions. Ozaki et al. [7] analyzed the boundary effects of friction on disc springs using a nonlinear finite element method, proposing a simplified design method based on energy equivalence and friction laws to predict the load-deflection curve and extending its application to stacked and juxtaposed disc springs. Zhou et al. [8] established a mechanical model of disc springs considering asymmetric friction boundaries and derived an additional load to overcome Coulomb friction damping using the energy method. Chaturvedi et al. [9] analyzed the impact of stepped sections on the load-deflection and variable stiffness characteristics, proposing a simplified method to predict the load deflection of stepped disc springs combined with geometric nonlinearity. Li et al. [10] developed a predictive model for the load-deflection of disc springs in contact with different fractal surfaces, using the fractal coefficient of static friction to replace Coulomb's law, based on contact mechanics and fractal theory. Chen et al. [11, 12] created a nonlinear model considering friction stiffness and contact stiffness using the energy method to study the load-deflection relationship and stiffness characteristics of disc springs under different contact conditions. Xu et al. [13] examined the influence of varying edge support surface widths on the mechanical properties of disc springs, comparing existing bearing capacity prediction formulas. Numerical simulations and experimental results led to the correction of standard bearing capacity calculation formulas, verifying their accuracy.

Regarding the application of combined disc springs in different working conditions, Zhou et al. [14] studied the influence of constraint mode and the number of disc springs on the dynamic characteristics of the disc spring system through simulation and experiment, and obtained the amplitude and amplification factor of the disc spring system under different constraint modes and different numbers of disc springs. Zhao et al. [15] proposed to arrange multiple shape memory alloy disc spring pieces in parallel to form a disc spring group. Through experiments, it was found that the number of disc spring pieces has little effect on the overall recovery deformation of the disc spring group, but has a linear effect on the ultimate bearing capacity and secant stiffness, indicating that the number of pieces does have an impact in a certain model. Shi et al. [16], in order to ensure that the hydraulic jacking device can provide sufficient sealing force, used ANSYS software to analyze different combination types with disc springs as the object. They found that the maximum stress is located at the inner hole of the upper surface, and the optimal disc spring combination type was obtained based on the stress. Chen et al. [17] proposed a metal energy-dissipating damper with a self-reset function. The influence of the initial pre-pressure, equivalent stiffness, and yield strength of the composite combination type disc spring of the damper on the seismic performance was studied by experimental methods, providing a theoretical basis and experimental proof for the design and application of metal energy-dissipating dampers, and providing an important reference for the improvement and optimization of seismic performance. Zhu et al. [18] designed a low-frequency passive vibration isolation system with parallel positive and negative stiffness. In this system, disc springs and rectangular springs are combined in parallel for optimal performance. After simulation and experimental research, the positive and negative stiffness parallel vibration isolation system achieved good vibration isolation performance. Li et al. [19], through the research on a new type of prestressed disc spring self-reset reinforced concrete pier (PDS-SCCP), found that the plastic damage mainly concentrated in the replaceable disc spring part, while the concrete pier body basically remained elastic. Therefore, the function of the disc spring device is to provide restoring force for the pier, and the performance of the disc spring structure determines the self-reset function of the pier. Lu et al. [20] proposed a three-dimensional vibration and shock dual-control support based on rubber isolation bearings and disc springs. The study found that the horizontal direction where the rubber bearing is located has a significant vibration isolation effect, and the vibration level in the vertical direction where the disc spring is located is also significantly reduced, proving the effectiveness of the three-dimensional vibration and shock dual-control support based on rubber isolation bearings and disc springs in the subway superstructure. Kang et al. [21] studied a new three-dimensional vibration isolation device, and analyzed disc springs with different combinations when designing the disc spring vibration isolation device. They found that the vertical damping is entirely provided by the viscous damper in parallel with the disc spring, and the disc spring combination method also has a significant impact on the vibration absorption effect. Chen et al. [22] proposed a load-adaptive quasi-zero stiffness vibration isolation system with multiple face-to-face disc springs and helical springs in parallel. The stiffness of the negative stiffness structure is reduced by changing the disc spring combination method. Chen et al. [23], through the research on the disc spring-based self-reset energy-dissipating brace (SCED), quantified the friction effect of the combined spring by the incremental energy method through multi-stage parallel stacking of disc springs and the composite of new and old springs, and its combination method has an impact on the friction effect. Jia et al. [24] established a finite element model of a vibration isolator with combined disc springs. By comparing simulation calculation and experimental research results, it was found that the combined (i.e., the overall structure non-linearly combined by disc springs) vibration isolator has the best vibration isolation performance. Zheng et al. [25] established a mathematical model for a non-linear combined disc spring vibration isolator, studied the simulation results of the combined vibration isolator under simple harmonic excitation, and found that the damping ratio and load type all have an impact on the vibration isolator. Based

on this result, a solid theoretical foundation was laid for the parameterization and serialization design of non-linear combined disc spring vibration isolators. The above scholars have discussed the combination types of disc spring components in the structure of devices in different fields, including the combination of the disc spring's own structure and the combination of the disc spring with other components, showing the diversification of combination types and effectively improving the performance. However, different combination types, different friction coefficients, and the contact nonlinearity of combined disc springs still need to be considered for actual working conditions. In addition, there is little research in the literature on the influence of the number of disc spring pieces in combined disc springs, which is also a necessary component parameter in the combination type of disc springs.

This paper intends to study the disc spring assemblies in disc spring bellows. Firstly, matching composite disc springs are selected based on the parameters and working conditions of the bellows. Then, considering the impact of friction on disc spring loads, experiments and numerical simulations with different friction coefficients are conducted. The accuracy of the numerical model for composite disc springs with different numbers of discs are verified against experimental results. The frictional impact on disc spring loads from previous studies are used to fit empirical formulas for different disc numbers in composite disc springs.

2. MATERIAL AND METHODS

2.1 Constructing the Mechanical Model of the Disc Spring Bellows

The disc spring bellows rely on pre-compressed disc springs to balance the blind flange force generated by the internal pressure of the pipeline. The main components include the bellows, guide rod, flange, nut, and disc spring assembly (as shown in Figure 2(a)). Before operation, the disc spring assembly undergoes pre-compression. This is achieved by fixing the extended length of the guide rod with a nut, allowing the disc spring assembly to both compress and extend. In the initial state, the disc spring assembly is as shown in Figure 2(b). When the bellows are subjected to an external load, P , the bellows are compressed, resulting in a displacement, f . The guide rod moves downward with the bellows, and the disc spring assembly is released, causing the disc springs to be stretched, with a displacement also equal to f (as shown in Figure 2(c)). Conversely, when the bellows are stretched, the disc springs are compressed. The working principle of the disc springs is to generate an equal and opposite reactive force through their deformation to balance the force on the bellows.

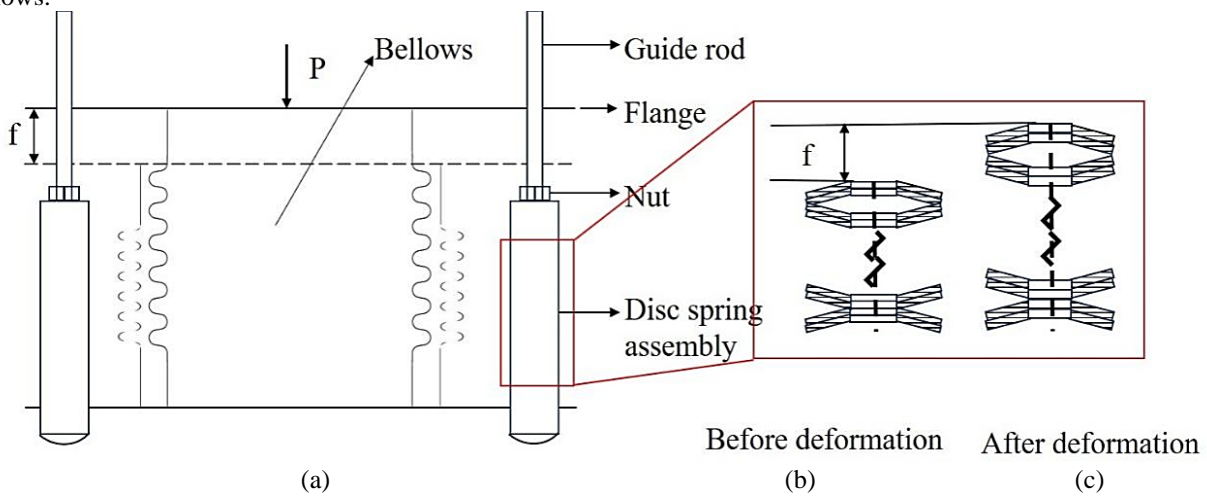


Figure 2. Model of the disc spring and bellows

The structure of the disc spring bellows mainly consists of the bellows and the disc spring assembly, as shown in Figure 2(a). The structural parameters of the bellows are listed in Table 1.

Table 1. Structural parameters of metal bellow

Parameter	Bellows Root Diameter, D_b (mm)	Design Pressure, p_1 (MPa)	Operating Pressure, p_2 (MPa)	Wave Height, h (mm)	Wave Pitch, q (mm)	Single Layer Thickness, δ (mm)	Number of Layers n	Number of Waves N
Value	500	0.67	0.4	38.5	50	1.5	1	6

According to [26], the effective area of the bellows is calculated:

$$A = \frac{\pi}{4} \cdot (D_b + h + n\delta)^2 = 228598.19 \text{ mm}^2 \tag{1}$$

The pressure thrust (design pressure) of the bellows, with a design pressure of 0.67 MPa:

$$F_{p1} = p_1 \cdot A = 137158.9 \text{ N} \tag{2}$$

Select composite disc springs from the A series with $D = 71$ mm. Each composite group consists of 2 disc springs. The load per single disc spring:

$$P_1 = \frac{4E}{1 - \mu^2} \cdot \frac{t^4}{k_1 D^2} \cdot k_4^2 \cdot \frac{f}{t} \left\{ k_4^2 \left(\frac{h_0}{t} - \frac{f}{t} \right) \cdot \left(\frac{h_0}{t} - \frac{f}{t} \right) + 1 \right\} = 17144.9 \text{ N} \tag{3}$$

$$P_c = 4E \cdot h_0 \cdot k_4^2 / [(1 - \mu^2) \cdot k_1 \cdot D^2] = 26657.5 \text{ N} \tag{4}$$

and,

$$P_1/P_c = 0.64 \tag{5}$$

$$f_1/h_0 = 0.64 \tag{6}$$

$$f_1 = 2.2 \times 0.78 = 1.04 \text{ mm} \tag{7}$$

The pressure thrust (operating pressure) of the bellows, with an operating pressure of 0.4 MPa:

$$F_{p2} = p_2 \cdot A = 91439.2 \text{ N} \tag{8}$$

Selecting composite disc springs from the A71 series and each composite group consists of 2-disc springs, the load per single disc spring:

$$P_2 = \frac{4E}{1 - \mu^2} \cdot \frac{t^4}{k_1 D^2} \cdot k_4^2 \cdot \frac{f}{t} \left\{ k_4^2 \left(\frac{h_0}{t} - \frac{f}{t} \right) \cdot \left(\frac{h_0}{t} - \frac{f}{t} \right) + 1 \right\} = 11429.9 \text{ N} \tag{9}$$

$$P_c = 4E \cdot h_0 \cdot k_4^2 / [(1 - \mu^2) \cdot k_1 \cdot D^2] = 26657.5 \text{ N} \tag{10}$$

$$P_2/P_c = 0.43 \tag{11}$$

Similarly, from [26]:

$$f_2/h_0 = 0.43 \tag{12}$$

$$f_2 = 2.2 \times 0.58 = 0.688 \text{ mm} \tag{13}$$

According to the requirement for a total deformation of 20 mm for the bellows, the number of composite groups needed is:

$$i = 10/f_1 - f_2 = 28 \tag{14}$$

Therefore, 28 composite groups of disc springs are required (equivalent to 56 individual discs).

2.2 Experimental Setup

2.2.1 Bellows parameters

On the universal testing machine, a tensile-compression test was conducted on the 56 disc springs calculated earlier, with the disc spring structural parameters as shown in Table 2. The objective of the experiment is to measure the force-displacement curve of the disc spring assembly during tension and compression processes. The loading setup for the test, depicted in Figure 3(a), involves connecting the disc springs together via guide rods inside a sleeve to form the disc spring assembly. This setup serves to guide and prevent lateral sliding of the disc springs. The lower end is fixed to the base of the testing machine, while the upper end is connected to a sensor via a double-nut connection, and then the sensor is linked to the testing machine.

Loading conditions involve fixing the lower end and applying displacement load to the upper end. The applied displacement load on the testing machine corresponds to ± 10 mm displacement, reflecting actual displacements encountered in the operating conditions of the bellows. The testing machine will continuously collect real-time input displacement and output force data, obtaining the relationship curve between compression force and displacement for the disc spring assembly.

Table 2. Disc spring structural parameters

Parameter	Outer Diameter, D (mm)	Inner Diameter, d (mm)	Thickness, t (mm)	Free Height, H (mm)	Deformation, h (mm)
Value	71	36	4	5.6	1.4

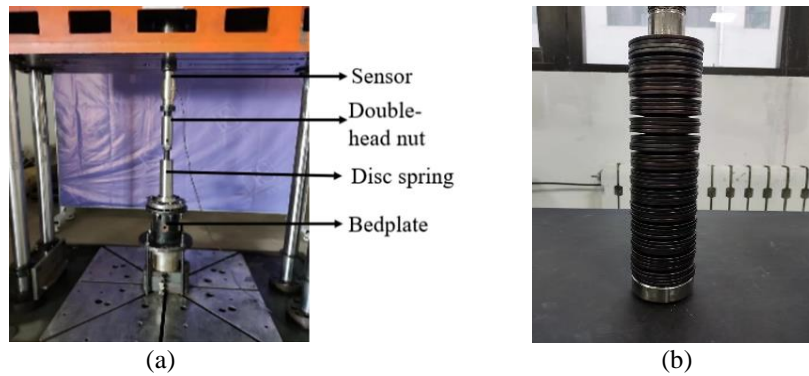


Figure 3. Disc spring assembly test setup: (a) Tensile-compression test loading setup and (b) Core of the spring assembly

2.3 Finite Element Modeling

2.3.1 Developing models of disc springs with different combinations

Disc springs, known for their small size, high load-bearing capacity, variable stiffness, and good self-centering capability, have garnered widespread attention in the field of engineering structures. Disc springs can be combined in various configurations to meet specific requirements for axial stiffness, deformation capacity, or load-bearing capacity. As shown in Figure 4(a) to 5(c), disc spring assembly methods include nesting, stacking, and composite configurations.

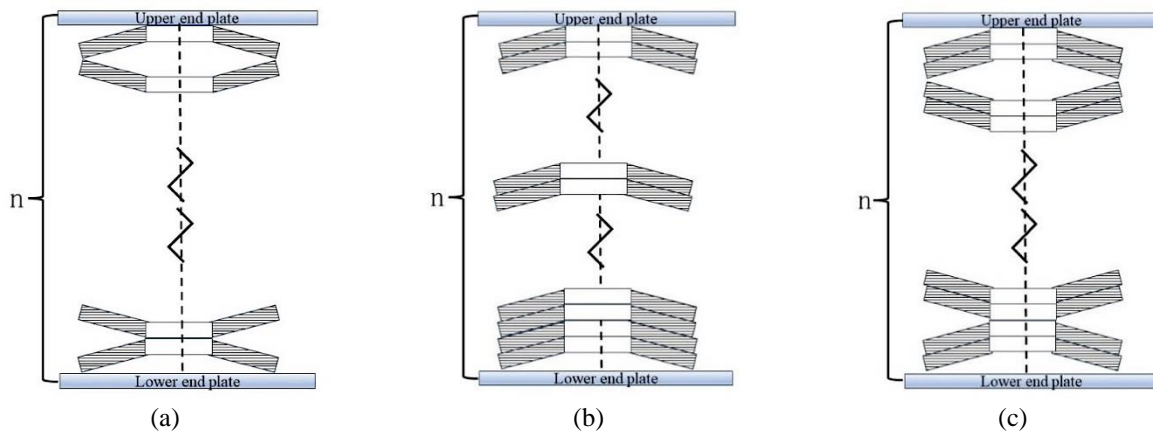


Figure 4. Different configurations of disc springs: (a) Nested, (b) Stacked and (c) Composite

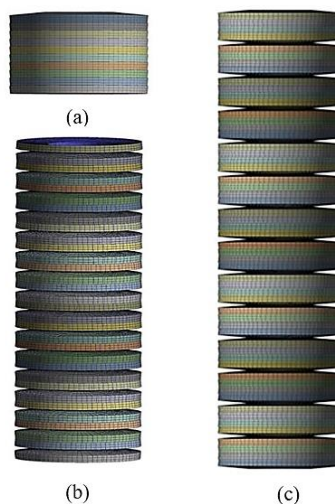


Figure 5. Disc spring models for different assembly methods: (a) nested, (b) stacked and (c) composite

For the three assembly methods, in finite element analysis to accurately simulate and compute, nested configuration disc springs were modeled with 1, 2, 4, 8, 16, and 32 discs; stacked configuration disc springs were modeled with 2 to 10 discs; composite configuration disc springs were modeled with 2, 4, 8, 16, 32, and 56 discs. Figure 5 illustrates the disc spring models for different assembly methods. After analyzing the mesh independence, the finite element model used a mesh density of 2 mm. At this scale, the finite element analysis of the disc spring models is relatively stable, improving analysis efficiency while ensuring computational accuracy.

3. RESULTS AND DISCUSSION

3.1 Experimental Test Results

Samples of three types of disc springs with different surface treatments were tested: galvanized, graphite-coated, and lubricated with frictionless oil, resulting in friction coefficients of 0.16, 0.1, and 0, respectively. Each condition underwent cyclic displacement of ± 10 mm in the test, resulting in load-displacement characteristic curves for different disc spring samples (see Figure 6).

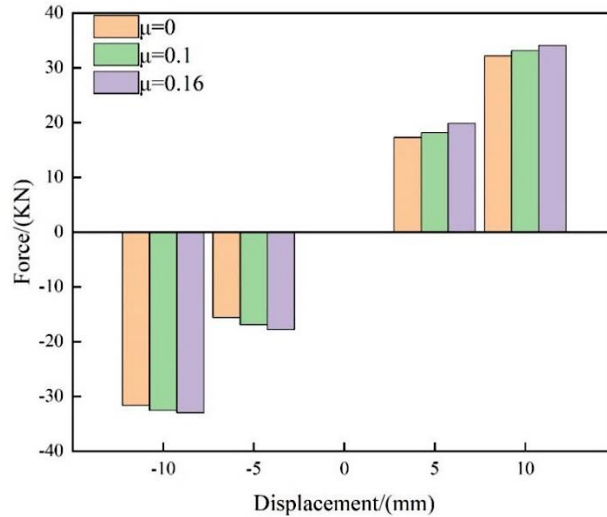


Figure 6. Force-displacement curves

From the values and trends in Figure 6, it is evident that with an increase in the friction coefficient (both in positive and negative directions), the load on the disc springs increases. This indicates that friction consistently impedes the loading-unloading process of the disc springs. The reason for this is that frictional force arises from the mutual rubbing between two contacting surfaces. As the disc springs compress or extend, the contact area between the discs increases, resulting in more frictional force being generated. According to the disc spring (GB/T 1972-2005) load calculation formula, theoretical load data for the disc springs are obtained. As shown in Table 3, with an increase in the friction coefficient, the calculated load results also increase. However, at a friction coefficient of 0, the load discrepancy between the two methods is 9%. At a friction coefficient of 0.16, this discrepancy reaches 22%. This phenomenon is attributed to external factors influencing the experiment, resulting in experimental errors. Additionally, friction's impact on disc springs is nonlinear; as the friction coefficient approaches a critical value, its effect on load variation decreases.

Table 3. Disc spring load data

Friction Coefficient, μ	0	0.1	0.16
Standard Calculation (N)	35061.4	38975	41739.8
Experimental Calculation (N)	32151.0	33092	34078.0

3.2 Calculation of Load for Nested Configuration Disc Springs

Nested configuration disc springs as shown in Figure 7 are used by connecting multiple disc springs in series. Their main advantages include increasing the overall deformation range and strain energy, making them suitable for applications requiring large deformations. The load calculation for nested configuration disc springs is according to [27]:

$$P_i = P \tag{15}$$

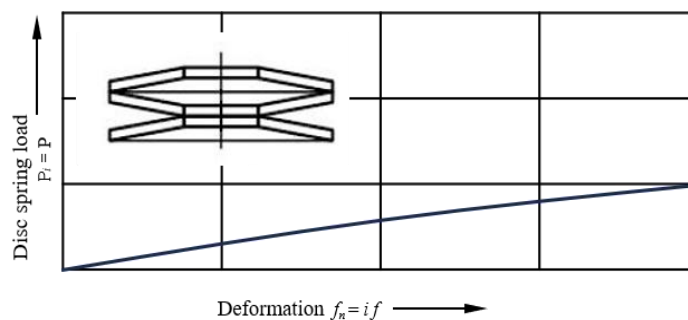


Figure 7. Nested configuration disc springs

In nested configuration disc springs, friction between the discs primarily arises from the contact edges of the inner and outer diameters. Compared to stacked configuration, the contact area can be negligibly small. Therefore, frictional

contact is typically assumed to be absent in the calculation of nested configuration disc springs. Simulation analysis was conducted on nested configuration disc springs with different numbers of discs. The displacement cloud map of the disc springs can be seen in Figure 8, revealing that under identical loading conditions, increasing the number of discs enhances the deformation capacity of the disc springs. The load diagram of the disc springs is shown in Figure 9, indicating that, without considering the influence of friction, the load of nested configuration disc springs does not increase with the number of discs. It remains essentially consistent with the load of a single-disc spring, aligning with the previously mentioned calculation results.

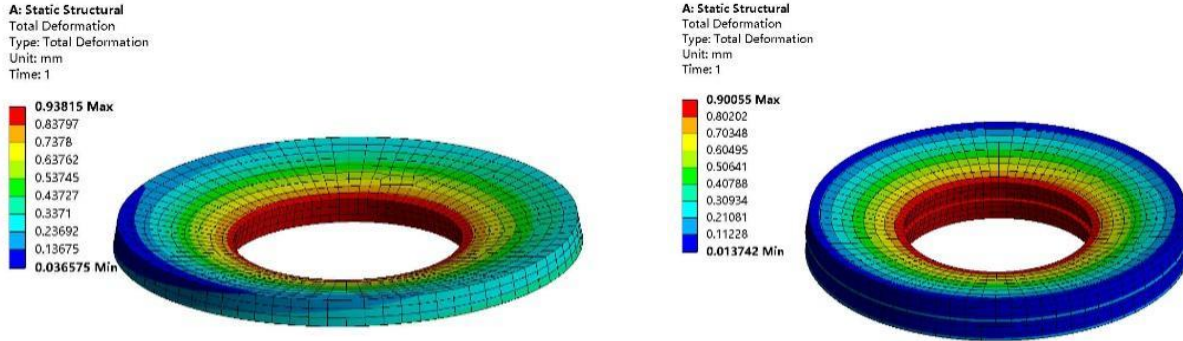


Figure 8. Disc spring displacement cloud map

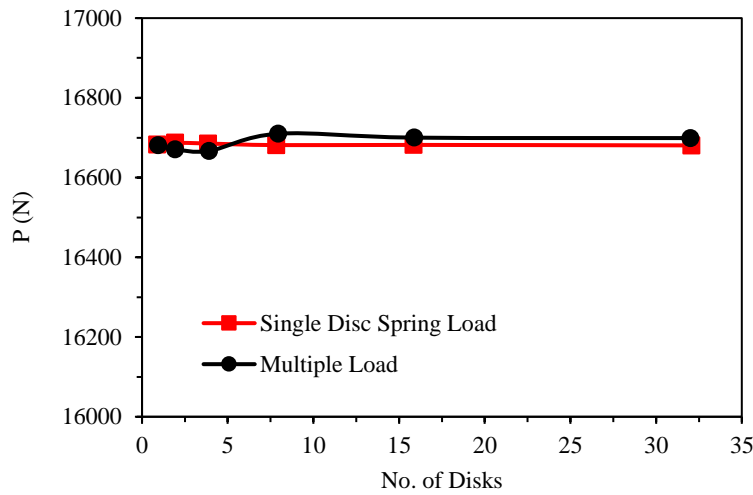


Figure 9. Load calculation of nested disc springs with different numbers of discs

3.3 Composite Stack Disc Spring Load Calculation

Stacked configuration disc springs as shown in Figure 10 are used by connecting multiple disc springs in parallel, forming a parallel structure. Their main advantages include increasing the overall load-bearing capacity and stiffness, making them suitable for applications requiring heavy loads. The load calculation for stacked configuration disc springs is:

$$P_n = n \cdot P \tag{16}$$

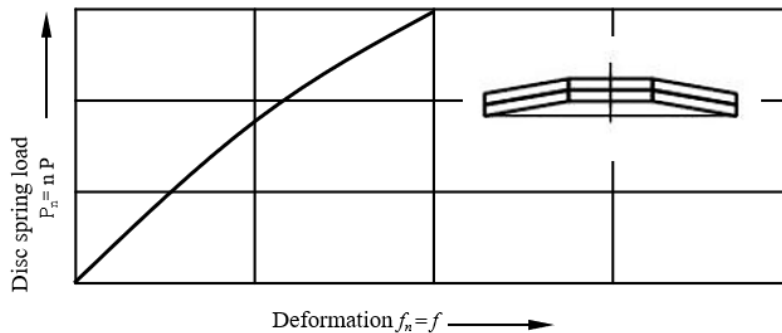


Figure 10. Stacked configuration disc springs

For stacked configuration disc springs, the influence of friction is significant due to the large contact area between the discs. Therefore, when establishing the disc spring model, it is necessary to consider the friction effects between the

conical surfaces of the stacked disc springs. Different numbers of discs (2 to 10 discs) were chosen for the stacked disc spring model, with varying friction coefficients set accordingly. From Figure 11, it can be observed that upon initial compression to the working position, the outer edge of the disc spring exhibits a region of minimum von Mises equivalent stress. This region extends axially towards both sides, with the von Mises stress gradually increasing. The maximum von Mises equivalent stress in the disc spring occurs at the inner edge of the disc spring's inner diameter, where the edge enters plastic deformation first during loading. Due to the Von Mises equivalent stress near this region reaching the material's maximum stress value, this area and its adjacent regions actually lose their load-bearing capacity first.

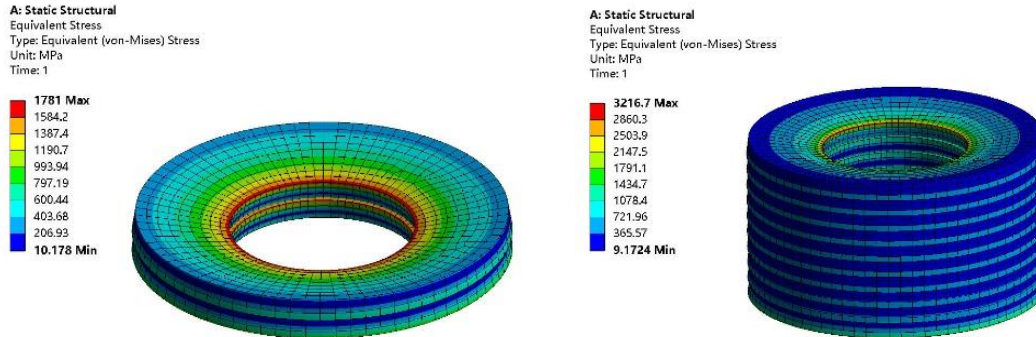


Figure 11. Equivalent von Mises stress plot of disc springs under different numbers of discs

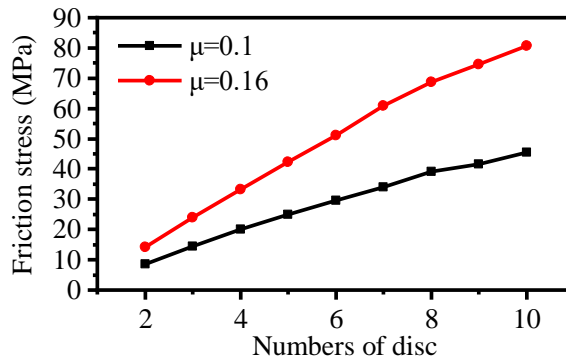


Figure 12. Friction stress plot of disc springs with different numbers of discs

From Figure 13, it is evident that as the number of discs in stacked disc springs increases, the overall load also increases. This is because the load in a stacked disc spring system is the sum of the loads on each disc. As the number of discs in stacked configuration increases, the load-displacement curve of the system also changes. With an increase in both the friction coefficient and the number of discs, the difference in disc spring loads also increases. Under conditions with a friction coefficient of 0.16, the load for two discs is 32,898 N, which is 3.7% higher compared to the situation without friction. For ten discs, the load is 165,780 N, marking a 27% increase compared to the frictionless scenario, with the difference increasing by 23.3%. This increase is due to the greater number of discs increasing the contact surfaces, resulting in cumulative frictional effects on each contact surface.

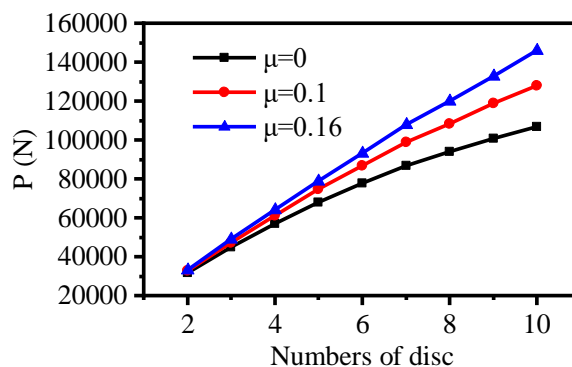


Figure 13. Load diagram of stacked disc springs with different numbers of discs

3.4 Composite Stack Disc Spring Load Calculation

In consideration of the advantages and disadvantages of nested and stacked configurations of disc springs in engineering applications, a combined approach known as composite configuration disc springs (as shown in Figure 14) has been adopted. This configuration combines the strengths of both by offering the capability to withstand significant

loads while also providing substantial deformation capacity. The load calculation for composite configuration disc springs is:

$$P_n = n \cdot P \tag{17}$$

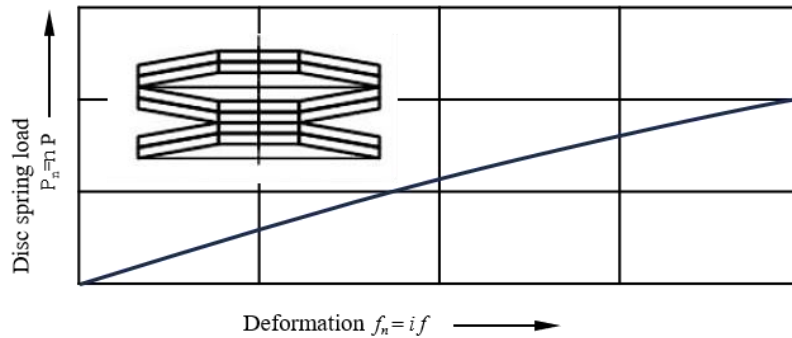


Figure 14. Composite configuration disc springs

Based on the analysis results of nested and stacked configuration disc springs, in composite configuration disc springs, only the contact friction between the stacked surfaces is considered. The friction coefficients are based on experimental treatments: zinc-plated surface, graphite coating, and no friction consideration (coefficients chosen as 0.16, 0.1, and 0, respectively). These scenarios are applied to analyse pairs of two-disc composite configuration disc springs using geometric models. From Figure 15, it can be observed that as the number of disc spring layers increases, the load of the disc spring increases with the increase in friction coefficient. With more layers of disc springs, the contact surfaces also increase, thereby amplifying the influence of surface friction. At $\mu = 0.16$, the load for 8 layers of disc springs is 33509 N, which corresponds to a load increase of 0.009 compared to two layers of disc springs. For 56 layers of disc springs, the load is 34070 N, indicating a load increase of 0.02 relative to two layers of disc springs. This demonstrates that as the number of disc spring layers increases, the cumulative effect of friction on the contact surfaces also increases. The relative load increase rate is 0.011 for 8 layers of disc springs, and after exceeding 8 layers, the influence of friction on the load stabilizes.

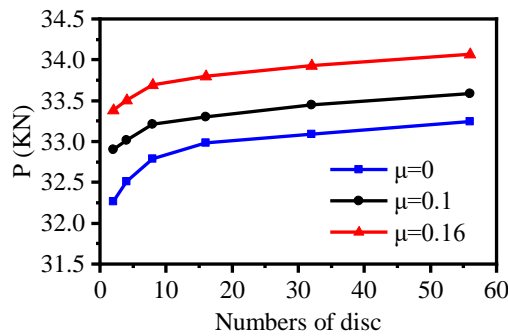


Figure 15. Effect of friction on load for pairs of two-disc configurations with different numbers of groups

Table 4 presents the data for the calculation and experimental results of 56 composite disc springs. A comparison reveals that when the friction coefficient is 0, the numerical calculation results differ from the experimental results by 3.3%. When the friction coefficient is 0.1, the numerical calculation results differ from the experimental results by 1.5%. When the friction coefficient is 0.16, the numerical calculation results differ from the experimental results by 1.4%, confirming the accuracy of the model.

Table 4. Experimental Results and Numerical Calculation Data

Friction coefficient, μ	0	0.1	0.16
Numerical calculation (N)	33252	33588	34570
Experimental results (N)	32151	33092	34078

In the previous phase of our work, we conducted a detailed study on the load prediction model for two-layer composite disc springs under different load friction conditions, with the calculation formula referenced as [28]:

$$P_\mu = \frac{P}{1 - \mu \left(\frac{5.6 - f}{35} \right)} \tag{18}$$

Based on the comparison between numerical calculations and experimental results, the calculation errors are within an acceptable range, thereby confirming the accuracy of the disc spring model in this study. Building upon this foundation,

our research extended to multi-layer composite disc springs. Further adjustments were made to the above model based on numerical calculation results, yielding the following outcome:

$$P_{n\mu} = P_{\mu} + 1031.97 \left(1 - e^{-\frac{n}{4}}\right) + 8.9 \left(1 - e^{-\frac{n}{14}}\right) \quad (19)$$

Building upon the foundation of two-layer composite disc springs, we have also established a three-layer composite disc spring configuration. Figure 16 depicts the load analysis of a three-layer composite disc spring under varying numbers of discs based on friction effects. As the number of discs increases, the trend of change is similar to that of the two-layer configuration, but its nonlinearity becomes more pronounced.

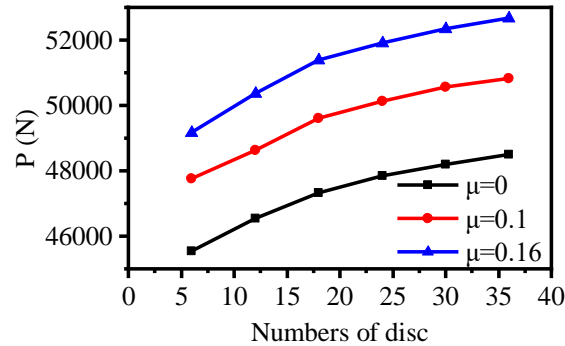


Figure 16. Influence of friction with different numbers of discs in a three-layer composite disc spring on load

4. CONCLUSIONS

This paper focuses on the study of disc spring bellows, calculating the combination forms of disc springs based on bellows parameters and operational requirements. Subsequently, different friction analyses were conducted on these composite disc springs. Experimental results on composite disc springs revealed discrepancies between the impact of friction on load compared to theoretical calculations. Parameter analyses of frictional effects were performed using numerical simulations, and the accuracy of the proposed calculation methods was validated against experimental results of composite disc springs. The main conclusions are as follows:

- i) The stroke of the disc spring increases proportionally with the number of overlapping discs. In composite disc springs, the frictional effect on the surface increases exponentially with the number of discs.
- ii) Based on data from numerical calculations and experimental results of 56 composite disc springs, comparisons showed that when the friction coefficient is 0, the relative difference between numerical calculations and experimental results is 3.3%; when the friction coefficient is 0.1, the relative difference is 1.5%; and when the friction coefficient is 0.16, the relative difference is 1.4%, confirming the model's accuracy.
- iii) For composite disc springs composed of two discs per group, modifications were made to the load prediction model considering the influence of different frictions. The revised prediction model provides guidance for selecting disc springs in bellows.

This study investigated the relationship between the number of discs per group and load in composite disc springs with two discs per group, resulting in a reliable load prediction model. However, applying this model to composite disc springs with three discs per group showed larger prediction errors, attributed to increasingly pronounced nonlinearity in load as the number of discs per group increases. Addressing this phenomenon, further research will be conducted in future work.

ACKNOWLEDGEMENTS

This work was supported by Fundamental Research Project (No. LJ212410154034) of the Educational Department of Liaoning Province.

CONFLICT OF INTEREST

The authors declare no competing interests.

AUTHORS CONTRIBUTION

Y. Ma (Conceptualisation; Methodology; Investigation; Writing - review & editing; Funding acquisition)

S. Li (Conceptualisation; Methodology; Validation; Formal analysis; Data curation; Writing - original draft; Visualisation)

T. Su (Conceptualisation; Methodology; Investigation; Writing - review & editing; Visualisation)

Q. Yuan (Validation; Methodology; Supervision)

Z. Song (Validation; Methodology; Supervision)

X. Li (Validation; Software; Supervision)

AVAILABILITY OF DATA AND MATERIALS

The data supporting this study's findings are available on request from the corresponding author.

ETHICS STATEMENT

Not applicable.

REFERENCES

- [1] Z. Wang, X. Wang, "Elastoplastic finite element analysis of disc spring," *Aerospace Manufacturing Technology*, vol. 2018, no. 2, pp. 19-22, 2018.
- [2] D. Zhu, F. Ding, H. Liu, S. Zhao, G. Liu, "Mechanical property analysis of disc spring," *Journal of the Brazilian Society of Mechanical Sciences and Engineering*, vol. 40, no. 230, pp. 1-12, 2018.
- [3] J. O. Almen. A. Laszlo., "The uniform-section disk spring," *Transactions of the American Society of Mechanical Engineers*, vol. 4, pp. 305-314, 1936.
- [4] G. Curti, R. Montanini, "On the influence of friction in the calculation of conical disk springs," *Journal of Mechanical Design*, vol. 121, no. 4, pp. 622-627, 1999.
- [5] S. Ozaki, K. Tsuda, J. Tominaga, "Analyses of static and dynamic behavior of coned disk springs: Effects of friction boundaries," *Thin-Walled Structures*, vol. 59, pp. 132-143, 2012.
- [6] N. P. Mastricola, "Nonlinear stiffness and edge friction characterization of coned disk springs," *Ph.D. Thesis*, The Ohio State University, United States, 2016.
- [7] N. P. Mastricola, J. T. Dreyer, R. Singh, "Analytical and experimental characterization of nonlinear coned disk springs with focus on edge friction contribution to force-deflection hysteresis," *Mechanical Systems and Signal Processing*, vol. 91, pp. 215-232, 2017.
- [8] Y. Zhou, D. Wang, Z. Qiu, Z. Wei, W. Chen, R. Zhu, "Modeling of disc springs based on energy method considering asymmetric frictional boundary," *Thin-Walled Structures*, vol. 190, p. 110971, 2023.
- [9] R. Chaturvedi, M. Trikha, K. R. Y. Simha, "Theoretical and numerical analysis of stepped disk spring," *Thin-Walled Structures*, vol. 136, pp. 162-174, 2019.
- [10] X. Li, R. Chen, Z. Yang, H. Yang, J. Xu, "Static behavior analysis of disc spring considering variable static friction coefficient," *Proceedings of the Institution of Mechanical Engineers, Part C: Journal of Mechanical Engineering Science*, vol. 235, no. 21, pp. 5583-5593, 2021.
- [11] R. Chen, X. Li, J. Xu, Z. Yang, H. Yang, "Properties analysis of disk spring with effects of asymmetric variable friction," *International Journal of Applied Mechanics*, vol. 13, no. 7, p. 2150076, 2021.
- [12] R. Chen, X. Li, Z. Yang, J. Xu, H. Yang, "Nonlinear behavior of disk spring with complex contact state," *Science Progress*, vol. 104, no. 4, pp. 1-27, 2021.
- [13] L. Xu, F. Yang, P. Chen, X. Xie, "Calculation method of bearing capacity of disc springs considering the width of the bearing surface," *Engineering Mechanics*, vol. 12, pp. 1-11, 2024.
- [14] J. Zhou, C. Zhang, Z. Wang, K. Mao, X. Wang, F. Minghini, "A study on the influence of different constraint modes and number of disc springs on the dynamics of disc spring system," *Shock and Vibration*, vol. 2021, pp. 1-12, 2021.
- [15] Q. Zhao, Z. Sun, Z. Tan, "Cyclic compression performance of SMA disc spring groups and a simplified model," *Engineering Mechanics*, vol. 41, no. 7, pp. 163-175, 2024.
- [16] D. Shi, G. Lin, S. Gao, H. Wang, "Numerical simulation and analysis of different combination types of hydraulic jacking tensioner disc springs," *Machine Tools & Hydraulics*, vol. 49, no. 4, pp. 155-159, 2021.
- [17] Y. Chen, C. Chen, Z. Xu, "Study on seismic performance of metal energy-dissipating damper with self-centering function," *Vibration and shock*, vol. 40, no. 23, pp. 25-31, 2021.
- [18] L. Zhu, T. Zhou, Y. Wu, H. Bai, Y. Tang, "Modeling and performance analysis of positive and negative stiffness parallel vibration isolation systems," *Noise and Vibration Control*, vol. 42, no. 5, pp. 268-273, 2022.
- [19] C. Li, H. Jia, Y. Li, J. Wang, "Study on the restoring force model and hysteretic performance of self-centering

- reinforced concrete piers with preloaded disc springs," *World Earthquake Engineering*, vol. 40, no. 1, pp. 164-174, 2024.
- [20] D. Lu, Y. Zhou, R. Wang, K. Ma, L. Wang, "Study on the damping effect of three-dimensional vibration dual control support in subway superstructure structure," *Structural Engineer* vol. 40, no. 1, pp. 11-21, 2024.
- [21] B. Kang, J. Wang, Z. Wang, "Study on vertical seismic performance of long-span continuous beam bridge," *Inner Mongolia Roads and Transport*, vol. 2024, no. 1, pp. 38-42, 2024.
- [22] L. Chen, M. Li, C. Zheng, G. Xu, L. Hu, Q. Ji, "Design and characterization of load adaptive quasi-zero stiffness vibration isolation system," *Chinese Journal of Applied Mechanics* pp. 1-10, 2024.
- [23] P. Chen, L. Xu, X. Xie, "Enhanced design and experimental investigation of disc spring-based self-centering buckling-restrained braces with a compounded combination mode," *Earthquake Engineering & Structural Dynamics*, vol. 52, no. 10, pp. 3053-3073, 2023.
- [24] F. Jia, F. Y. Xu, "Combined vibration isolator of disc springs for closed high-speed precision press: Design and experiments," *Transactions of the Canadian Society for Mechanical Engineering*, vol. 38, no. 4, pp. 465-485, 2014.
- [25] E. L. Zheng, F. Jia, Z. S. Zhang, J. F. Shi, "Modeling and simulation of nonlinear combination disc-spring vibration isolator for high-speed press," *Advanced Materials Research*, vol. 211-212, pp. 40-47, 2011.
- [26] GB/T1972-2005, "Disc spring," *China Standard Publishing House*, China, 2005.
- [27] W. Xiaobo, "Study on mechanical properties of disc springs," *Master Thesis*, Zhengzhou University, China, 2007.
- [28] Y. Ma, S. Li, T. Su, Z. Yang, Z. Mao, Q. Yuan, "Influence of fractal-based contact friction coefficient on the stiffness of disc springs: Experimental and numerical studies," *Proceedings of the Institution of Mechanical Engineers, Part C: Journal of Mechanical Engineering Science*, vol. 238, no. 18, pp. 9187-9199, 2024.